JOURNAL OF GUIDANCE, CONTROL, AND DYNAMICS
Vol. 39, No. 9, September 2016

Stochastic Cooperative Interception Using Information Sharing Based on Engagement Staggering

Vitaly Shaferman*
Technical University of Vienna, 1040 Vienna, Austria
and
Yaakov Oshman†
Technion–Israel Institute of Technology, 32000 Haifa, Israel

DOI: 10.2514/1.G000437

A novel cooperative tracking and interception strategy, which exploits information sharing and missile staggering, is presented. The key idea underlying the approach is to exploit the superior information collected by the leading missile to improve the interception performance of the trailing missiles. For tracking a maneuvering target, the paper derives a nonlinear adaptation of an interacting multiple model filter in cooperative and noncooperative estimation modes. The optimal staggering between the missiles is derived based on a linear model and a deterministic approximation of the stochastic estimation process. An extensive Monte Carlo study, in a nonlinear two-dimensional simulation of a ballistic missile defense scenario, is used to demonstrate the viability of the proposed strategy. It is shown that, for a two-on-one interception engagement, the trailing missile's estimation performance, in the information-sharing mode, substantially improves, when compared to that of noncooperating missiles. Combining this estimation improvement with guidance laws that use target acceleration yields a dramatic improvement in the team's closed-loop interception performance.

I. Introduction

THE most currently used guidance laws for interceptor missiles have been developed by assuming perfect information about the target's states. Using this assumption alongside additional assumptions, like linearization around a collision triangle and constant target and interceptor speeds, enables a simple mathematical formulation of the problem. Using this simplified model, the guidance problem can be formulated as an optimal control problem by assuming a known target strategy. For various target strategies and missile and target autopilot dynamics, this yields the well-known proportional navigation (PN) guidance law [1], the augmented PN (APN) guidance law [2], and the optimal guidance law (OGL) [3]. The simplified model can also be used to formulate a differential game in which no assumption on the future target strategy is made, resulting in the linear quadratic differential game (LQDG) guidance law [4] and the differential game guidance laws (DGL0, DGL1) [5,6]. Unfortunately, perfect information about the target's states is never available, and a special estimator is usually constructed to estimate these states. Several classes of estimators can be used to estimate the target's states in missile guidance scenarios. As most realistic targets are unpredictable, approaches that can address uncertainty in the target model (i.e., target maneuver) are usually used. In [7], a standard Kalman filter (KF), with a shaping filter representing the random target maneuver, was proposed. A multiple model adaptive estimator (MMAE) [8,9] can also be used if the unknown target maneuver belongs to a finite set of possible strategies [10,11]. In the MMAE approach, a bank of KFs is run in parallel, with each filter matching a different possible target strategy. This approach is also sometimes denoted the static multiple model.

Unlike the MMAE approach, in which each filter in the bank is matched with one fixed correct model throughout the scenario, the switching multiple model approach, sometimes denoted as the dynamic multiple model, assumes that different models can be correct at different times. This approach can be used if, at each time step, the target dynamics can be represented by a finite set of models, called modes, and the transition probability between these modes is known. Like in the MMAE approach, a bank of KFs is run in parallel with each filter representing a possible mode. One widely used algorithm belonging to this class is the interacting multiple model (IMM) filter [12,13], which was shown to achieve very good performance per computational complexity.

All the estimator classes presented thus far are based on the KF, which is the optimal estimator (in the MMSE sense) for linear and Gaussian estimation problems. The basic target-tracking problem is nonlinear, and the same approaches can be implemented using the extended Kalman filter (EKF) or the unscented KF to address the nonlinearity of the problem.

The target-tracking problem with application to missile guidance has been comprehensively studied in the past. Nevertheless, it seems that intercepting a highly maneuverable target in the presence of target maneuver uncertainty and noisy measurements is still limited by the estimator performance. Even when using state-of-the-art estimators, such as those mentioned previously, the estimate tends to exhibit a substantial time lag and significant tracking error. This, in turn, might result in poor interception performance against highly maneuverable targets. Most interception missiles are equipped with either an infrared (IR) sensor, which provides bearing-only measurements, or a radar sensor that provides bearing and range measurements. It is well known [14] that the most dominant estimation error in modern guidance laws that use target acceleration (like OGL and DGL1) is in the estimation of the target acceleration, for which the estimate is mainly inferred by the bearing measurement. Thus, the range measurement, available by radar seekers, does not alleviate this estimation limitation and does not improve interception performance when compared to IR sensors. In some scenarios, like the ballistic missile defense (BMD) scenario, it is common to launch more than one missile at high-valued targets (in order to increase interception probability), but the intercepting missiles do not typically cooperate or share any information. Thus, the available resources are not fully exploited. Cooperative interception in the perfect information setting

Presented as Paper 2009-5783 at the AIAA Guidance, Navigation, and Control Conference, Chicago, IL, 10–13 August 2009; received 26 January 2016; revision received 18 April 2016; accepted for publication 20 April 2016; published online 25 July 2016.

*Postdoctoral Fellow, Institute of Automation and Control; shaferman@acin.tuwien.ac.at.

†Professor, Dept. of Aerospace Engineering, Holder of the Louis and Helen Rogow Chair in Aeronautical Engineering; yaakov.oshman@technion.ac.il. Fellow AIAA.

has been extensively studied in recent years. Most of the research focused on guidance laws that enabled a team of interceptors to approach a target from different directions and/or at the same time [15–18]. However, the goal of these guidance laws is to saturate the target's defense systems and not to improve interception performance in a realistic noise-corrupted scenario. Thus, all of these laws exhibit degraded interception performance in a stochastic setting.

In [19], cooperative multiple model adaptive guidance for a defender missile protecting an airborne target is proposed. The target and its defender cooperatively identify the attacker's guidance law, estimate its states, and cooperate in guidance to minimize the defender's control effort. Although this work specifically includes cooperative estimation, it does not address the classic interception problem and is limited to a specific scenario in which the attacker chases one of the team members. In a recent paper [20] by the authors, an information-sharing estimation concept for combining the measurements from the intercepting missiles to improve target tracking, and consequently interception performance, is proposed. However, no logic for controlling the relative position between the missiles is proposed. The missiles are launched in a lateral separation mainly to improve the observability in range for an IR sensor.

This paper significantly extends the cooperative tracking concept of [20] by proposing a novel strategy consisting of the staggered launch of the missiles. Staggering the missiles has two potential benefits when compared to the nonstaggered case: a guidance benefit and an estimation benefit. The guidance benefit stems from the fact that, due to the time delay between the intercepts, an effective target evasive maneuver against one missile might turn out to be an ineffective evasive maneuver against the other missiles. This means that, to optimally evade the interceptor team, the target will have to forgo the optimality of its evasive maneuver against each one of the interceptors separately, resulting in a lower miss distance compared to an optimal evasion in a one-on-one setting. The estimation benefit stems from the fact that the leading missile acquires superior measurements, due to its closer range to the target, which it can share with the trailing missiles. The trailing missiles thus obtain a measurement of higher quality than they can collect with their own sensors, thus improving their estimation performance. Furthermore, because they are trailing, they have more time to react and correct any miss that might be induced by the target's evasive maneuver. This, in turn, leads to better interception performance if the target attempts to evade before the leading missile passes it. It is obvious that, to fully exploit these advantages, the staggering time between the missiles has to be optimized.

The remainder of this paper is organized as follows. The next section presents the mathematical models of the multiple missile guidance and estimation problem. The information-sharing EKF-based IMM target-tracking estimator is presented in Sec. III, followed by a presentation of the missile staggering strategy in Sec. IV, and a discussion of design considerations and implementation issues in Sec. V. A comparative simulation study is presented in Sec. VI, followed by concluding remarks.

II. Mathematical Model

We consider a scenario in which several missiles cooperatively track and intercept a single target. We assume that the missiles are guided to the target via a given guidance law, and that only the estimation and the decision regarding the missile staggering are performed cooperatively. This section presents the dynamics, measurement, and guidance models; and it addresses the assumptions taken in their derivation.

A. Nonlinear Kinematics and Dynamics

We consider skid-to-turn roll-stabilized missiles. The interception is assumed to transpire in the plane. In Fig. 1, a schematic view of the planar endgame geometry, for two intercepting missiles, is shown, where $X_I - O_I - Y_I$ is a Cartesian inertial reference frame. We denote time by the subscript t. Variables associated with the ith missile or the target are denoted by an additional subscript i or T, respectively, separated by a semicolon. M_i and T represent the ith missile and the target, respectively. The speed, normal acceleration, and

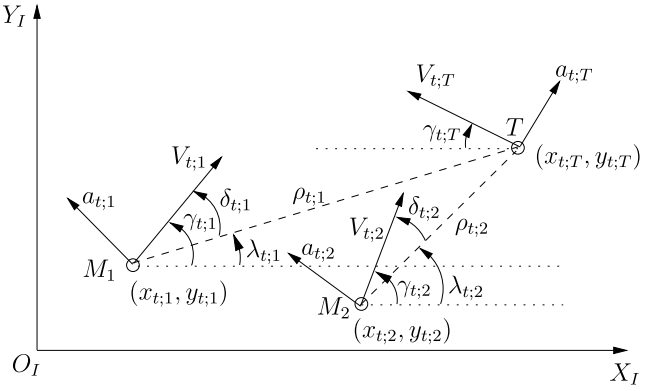

Fig. 1 Planar engagement geometry.

flight-path angles are denoted by V, a, and γ, respectively; the range between the ith missile and the target at time t is $\rho_{t;i}$, and $\lambda_{t;i}$ is the angle between the ith missile's line of sight (LOS) to the target and the X_I axis.

For the estimation, we assume that each missile's own inertial state vector at time t

$$\boldsymbol{x}^I_{t;i} = [\, x_{t;i} \quad y_{t;i} \quad \gamma_{t;i} \quad a_{t;i} \,]^T \tag{1}$$

is known to a very high accuracy (via some navigation system) and that each missile can transmit this state vector to the other missiles without any delays. For simulation purposes, we assume first-order lateral maneuver dynamics for the missiles. We also assume that the missiles move at a constant speed: $V_{t;i} = V_i$. Using these assumptions, the inertial state vector at time t of each missile can be calculated via

$$\dot{x}_{t;i} = V_i \cos(\gamma_{t;i}) \tag{2a}$$

$$\dot{y}_{t;i} = V_i \sin(\gamma_{t;i}) \tag{2b}$$

$$\dot{\gamma}_{t;i} = \frac{a_{t;i}}{V_i} \tag{2c}$$

$$\dot{a}_{t;i} = -\frac{a_{t;i}}{\tau_i} + \frac{u_{t;i}}{\tau_i} \tag{2d}$$

where τ_i is the time constant of the ith missile's dynamics; and $u_{t;i}$ is the ith missile's acceleration command at time t, which is dictated by its guidance law.

Most guidance laws are derived in relative polar coordinates. Therefore, each missile estimates the target's states in such a coordinate system. The ith missile's state vector of the target at time t is, therefore,

$$\boldsymbol{x}^R_{t;i} = [\, \rho_{t;i} \quad \lambda_{t;i} \quad \gamma_{t;T} \quad a_{t;T} \,]^T \tag{3}$$

which we will denote as $\boldsymbol{x}_t$ for the rest of the paper, to avoid excessive indexing.

Similar to the intercepting missiles, we also assume first-order lateral maneuver dynamics and constant speed $V_{t;T} = V_T$ for the target. Using these assumptions, the relative dynamic equations are

$$\dot{\rho}_{t;i} = V_{\rho i} \tag{4a}$$

$$\dot{\lambda}_{t;i} = \frac{V_{\lambda i}}{\rho_{t;i}} \tag{4b}$$

$$\dot{\gamma}_{t;T} = \frac{a_{t;T}}{V_T} \tag{4c}$$

$$\dot{a}_{t;T} = -\frac{a_{t;T}}{\tau_T} + \frac{u_{t;T}}{\tau_T} \tag{4d}$$

where

$$V_{\rho i} = -[V_{t;i}\cos(\delta_{t;i}) + V_T\cos(\delta_{t;Ti})] \tag{5a}$$

$$V_{\lambda i} = -V_{t;i}\sin(\delta_{t;i}) + V_T\sin(\delta_{t;Ti}) \tag{5b}$$

$$\delta_{t;i} = \gamma_{t;i} - \lambda_{t;i}, \quad \delta_{t;Ti} = \gamma_{t;T} + \lambda_{t;i} \tag{5c}$$

In Eq. (4), τ_T is the time constant of the target dynamics, and $u_{t;T}$ is the target's acceleration command at time t.

For simplicity of exposition, it is assumed that the target executes an evasion maneuver throughout the interception scenario. As is well known, the optimal perfect information evasion strategy has a bang–bang structure for bounded acceleration, games-based guidance laws [5,6], and linear guidance laws [21]. We therefore assume that the target applies, at any time, one of the following two possible commands:

$$u_{t;T} = \begin{cases} -a_T^{\max} & r = 1 \\ +a_T^{\max} & r = 2 \end{cases} \tag{6}$$

where $a_T^{\max}$ is the maximal target acceleration command, and r is the target mode. We assume that V_T, τ_T, and $a_T^{\max}$ are known parameters.

The discrete-time version of the equations of motion [Eq. (4)] can be generally described as

$$\boldsymbol{x}_k = \boldsymbol{f}_{k-1}(\boldsymbol{x}_{k-1}, r_k) \tag{7}$$

where $\boldsymbol{x}_k$ is the relative state vector of the ith missile at time t_k, $\boldsymbol{f}_{k-1}$ is derived by integrating Eq. (4) from t_{k-1} to t_k, and r_k is the mode in effect during the time interval $(t_{k-1}, t_k]$. The mode variable is modeled as a homogeneous Markov chain with transitional probabilities

$$\pi_{ij} = Pr\{r_k = j | r_{k-1} = i\}, \qquad (i, j \in S) \tag{8}$$

where $S \triangleq \{1, 2, \ldots, s\}$, $\pi_{ij} \geq 0$, and $\sum_{j=1}^{s} \pi_{ij} = 1$. In our model, the target has two possible modes; therefore, $s = 2$. These type of models are often referred to as discrete switching dynamics, jump Markov, or hybrid-state systems.

B. Measurement Model

As the bearing measurement is the dominant one in missile guidance applications, we assume that each missile is only equipped with an IR sensor, which measures the angle $\delta_{k;i}$ between the missile's velocity vector and the LOS to the target. The IR sensor's measurement is contaminated by measurement noise $v_{k;i}$, which is a zero-mean white Gaussian sequence with standard deviation σ_i. The measurement noises of the intercepting missiles are assumed to be mutually independent; therefore,

$$E(v_{k;i}v_{k;j}) = 0 \quad \forall\, i \neq j$$

For the case where the estimation is performed using own-missile measurements only (information nonsharing mode), the measurement equation of the ith missile is

$$z_{k;i} = h_k(\boldsymbol{x}_k) + v_{k;i} = \delta_{k;i} + v_{k;i} = \gamma_{k;i} - \lambda_{k;i} + v_{k;i} \tag{9}$$

where

$$v_{k;i} \sim \mathcal{N}(0, \sigma_i^2) \tag{10}$$

For the case where the estimation is performed using measurements from multiple missiles (information-sharing mode), the measurement equation is

$$\boldsymbol{z}_k = \begin{bmatrix} z_{k;1} \\ z_{k;2} \\ \vdots \\ z_{k;m} \end{bmatrix} = \boldsymbol{h}_k(\boldsymbol{x}_k) + \boldsymbol{v}_k \tag{11}$$

where m is the number of cooperating missiles; the measurement from the jth missile is expressed with the ith missile's relative state as

$$z_{k;j} = \gamma_{t;j} - \arctan\left[\frac{(y_{t;i} - y_{t;j}) + \rho_{t;i}\sin(\lambda_{t;i})}{(x_{t;i} - x_{t;j}) + \rho_{t;i}\cos(\lambda_{t;i})}\right] + v_{k;j} \tag{12}$$

and

$$\boldsymbol{v}_k = [v_{k;1}\ \ v_{k;2}\ \ \cdots\ \ v_{k;m}]^T \sim \mathcal{N}([0]_{m\times 1}, \boldsymbol{R}), \quad \boldsymbol{R} = \mathrm{diag}\{\sigma_1^2, \sigma_2^2, \ldots, \sigma_m^2\} \tag{13}$$

The objective of the estimator developed in this paper is to obtain filtered estimates of the relative state vector $\boldsymbol{x}_k$ based on the noisy measurement history $\mathcal{Z}_k \triangleq \{\boldsymbol{z}_l; l = 1, \ldots, k\}$ up to time k.

Remark 1: We choose the measurements to be $\delta_{k;i}$. This is not what the sensor will measure if the missile's angle of attack does not vanish (the sensor measures the angle between the boresight and the LOS), but the angle between the boresight and the flight path is typically known to a very good accuracy; therefore, it can easily be compensated for.

C. Filter Initialization

We assume that the filters in the missiles are initialized by the same radar. Figure 2 presents the planar geometry of the initializing radar and the ith missile. We denote variables associated with the radar by the subscript R. The range between the initializing radar and the target at time t is $\rho_{t;R}$, and $\lambda_{t;R}$ is the angle between the radar's LOS to the target and the X_I axis.

We assume that the radar measures the following initial state vector:

$$\hat{\boldsymbol{x}}_{0;R} = [\rho_{0;R} \quad \lambda_{0;R} \quad \gamma_{0;T} \quad a_{0;T}]^T \tag{14}$$

and passes on this measurement to the intercepting missiles at initialization. We also assume that the radar's position $(x_{0;R}, y_{0;R})$ is known and that the radar's measurement of the initial state vector is Gaussian and independent of the missiles' measurement noises:

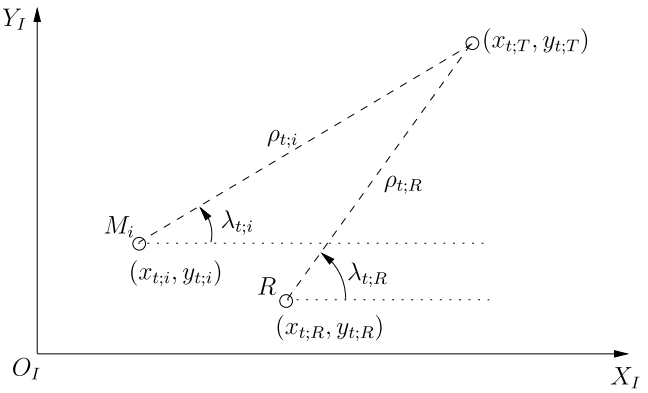

Fig. 2 Initializing radar geometry.

$$\hat{\boldsymbol{x}}_{0;R} \sim \mathcal{N}(\bar{\boldsymbol{x}}_{0;R}, \boldsymbol{P}_{0;R}) \tag{15}$$

The geometric relation between the ith missile's relative state vector and the radar's initial estimate is

$$\rho_{0;i} = \{\rho_{0;R}^2 + \Delta R_{Ri}^2 + 2\rho_{0;R}[\Delta X_{Ri}\cos(\lambda_{0;R}) + \Delta Y_{Ri}\sin(\lambda_{0;R})]\}^{1/2} \tag{16a}$$

$$\lambda_{0;i} = \arctan\left[\frac{\Delta Y_{Ri} + \rho_{0;R}\sin(\lambda_{0;R})}{\Delta X_{Ri} + \rho_{0;R}\cos(\lambda_{0;R})}\right] \tag{16b}$$

where

$$\Delta X_{Ri} \triangleq x_{0;R} - x_{0;i}; \quad \Delta Y_{Ri} \triangleq y_{0;R} - y_{0;i}; \quad \Delta R_{Ri} \triangleq (\Delta X_{Ri}^2 + \Delta Y_{Ri}^2)^{1/2} \tag{17}$$

D. Linearized Model Used for Guidance

As stated in the Introduction (Sec. I), most modern guidance laws are derived using linear models. We use such a model to present the missile guidance laws in Sec. IV.A and to derive the staggering strategy in Sec. IV.C.

Figure 3 shows a schematic view of the linearized planar endgame geometry of the ith missile and the target. The X_i axis, aligned with the LOS used for linearization, is denoted as LOS_{0i}. The relative displacement between the ith missile and the target normal to this direction is $\xi_{t;i}$. The missile and target accelerations normal to LOS_{0i} are denoted by $a_{t;i}^{n0}$ and $a_{t;Ti}^{n0}$, respectively, and satisfy

$$a_{t;Ti}^{n0} = a_{t;T}\cos(\delta_{0;Ti}), \qquad a_{t;i}^{n0} = a_{t;i}\cos(\delta_{0;i}) \tag{18}$$

The state vector of the linearized guidance problem for the ith missile is

$$\boldsymbol{y}_i = [\,\xi_{t;i} \quad \dot{\xi}_{t;i} \quad a_{t;i} \quad a_{t;T}\,]^T \tag{19}$$

Combining the linear kinematics and the ith missile's and target's first-order dynamics yields the linear equations of motion:

$$\dot{y}_1 = y_2 \tag{20a}$$

$$\dot{y}_2 = a_{t;Ti}^{n0} - a_{t;i}^{n0} = a_{t;T}\cos(\delta_{0;Ti}) - a_{t;i}\cos(\delta_{0;i}) \tag{20b}$$

$$\dot{y}_3 = -\frac{a_{t;i}}{\tau_i} + \frac{u_{t;i}}{\tau_i} \tag{20c}$$

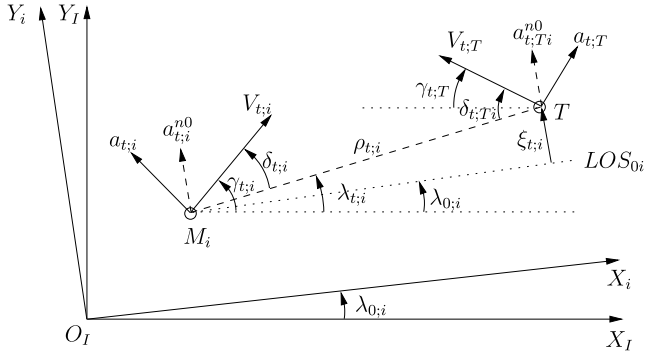

Fig. 3 Linearized planar engagement geometry.

$$\dot{y}_4 = -\frac{a_{t;T}}{\tau_T} + \frac{u_{t;T}}{\tau_T} \tag{20d}$$

III. Target-Tracking IMM Estimator

The IMM estimator is a well-known tool for estimating switching dynamics models [22,23]. In this section, we first present the generic IMM algorithm. We then derive a specific EKF-based IMM for the problem at hand. For simplicity of exposition, and with no loss of generality, a two-mode IMM estimator that matches the possible target modes as presented in Eq. (6) is derived. We note that the methodology developed herein is not limited to a specific type of estimator. More complex estimators, adapted to expected, more complex real-life target maneuvers, can certainly be used as warranted.

A. IMM Filter

The IMM filter [23] is designed to estimate switching dynamic models, like the model presented in Sec. II, in which the system dynamics have a known finite set of modes and can switch between these modes with a known transition probability. The filter runs a bank of KFs matched to the possible modes (a filter for each possible mode). The key idea is that the input to each filter is a combination of the previous mode-conditioned estimates. Each filter computes its state estimate, covariance, and likelihood. Using the likelihoods, previous step mode probabilities, and the known transition probabilities, the new mode probabilities are computed. These are used to compute the new mixing probabilities, the combined state estimate, and its covariance. We next present one cycle of the generic IMM estimation algorithm.

1. Mixing Probabilities

Conditioned on $\mathcal{Z}_{k-1}$, the probability that mode i was in effect at time $k-1$ given that mode j is in effect at time k is calculated via Bayes' rule as

$$\mu_{k-1}^{i|j} = Pr\{r_{k-1} = i | r_k = j, \mathcal{Z}_{k-1}\} = \frac{Pr\{r_k = j | r_{k-1} = i, \mathcal{Z}_{k-1}\}\mu_{k-1}^i}{Pr\{r_k = j | \mathcal{Z}_{k-1}\}} \tag{21}$$

where $\mu_{k-1}^i = Pr\{r_{k-1} = i | \mathcal{Z}_{k-1}\}$ is the ith mode-conditioned probability at $k-1$. Using the total probability theorem and the Markovian nature of the mode transition yields

$$\mu_{k-1}^{i|j} = \frac{\pi_{ij}\mu_{k-1}^i}{\sum_{i=1}^s \pi_{ij}\mu_{k-1}^i} \tag{22}$$

2. Initial Conditions

Theoretically, the initial conditions to each filter should be a Gaussian sum [weighted according to Eq. (22)]. However, as the KF requires Gaussian initial conditions, the algorithm approximates this sum using a single Gaussian probability density function via moment matching. The initial conditions of the jth filter are thus

$$\hat{\boldsymbol{x}}_{k-1|k-1}^{0j} = \sum_{i=1}^{s} \hat{\boldsymbol{x}}_{k-1|k-1}^i \mu_{k-1}^{i|j} \tag{23}$$

and the covariance matrix is

$$\boldsymbol{P}_{k-1|k-1}^{0j} = \sum_{i=1}^{s} \mu_{k-1}^{i|j}\{\boldsymbol{P}_{k-1|k-1}^i + [\hat{\boldsymbol{x}}_{k-1|k-1}^i - \hat{\boldsymbol{x}}_{k-1|k-1}^{0j}][\hat{\boldsymbol{x}}_{k-1|k-1}^i - \hat{\boldsymbol{x}}_{k-1|k-1}^{0j}]^T\} \tag{24}$$

where $\hat{\boldsymbol{x}}_{k-1|k-1}^i$ and $\boldsymbol{P}_{k-1|k-1}^i$ are the estimate and covariance, respectively, of the filter matched to the ith mode in the $k-1$ time step.

3. Model-Matched Filtering

Using the initial conditions of Eqs. (23) and (24), and the new measurement z_k, the estimate $\hat{\boldsymbol{x}}^j_{k|k}$, and the covariance $\boldsymbol{P}^j_{k|k}$ of the filter matched to the jth mode are computed using the standard KF equations.

The mode conditioned likelihood $\Lambda^j_k = p(z_k|r_k = j, \mathcal{Z}_{k-1})$ is calculated using the jth filter innovations process statistics. This likelihood is used in the next step to update the mode probabilities.

4. Mode Probability Update

The mode probability μ^j_k at time k is updated according to Bayes' rule:

$$\mu^j_k = Pr\{r_k = j|\mathcal{Z}_k\} = \frac{p(z_k|r_k = j, \mathcal{Z}_{k-1}) Pr\{r_k = j|\mathcal{Z}_{k-1}\}}{p(z_k|\mathcal{Z}_{k-1})} \tag{25}$$

Applying the total probability theorem yields

$$\mu^j_k = \frac{\Lambda^j_k \sum_{i=1}^s \pi_{ij}\mu^i_{k-1}}{\sum_{j=1}^s \Lambda^j_k \sum_{i=1}^s \pi_{ij}\mu^i_{k-1}} \tag{26}$$

5. Blended Estimation and Covariance

For output purposes, the mode-conditioned estimates and covariances are blended via the following mixture equations:

$$\hat{\boldsymbol{x}}_{k|k} = \sum_{j=1}^{s} \hat{\boldsymbol{x}}^j_{k|k}\mu^j_k \tag{27a}$$

$$\boldsymbol{P}_{k|k} = \sum_{j=1}^{s} \mu^j_k\{\boldsymbol{P}^j_{k|k} + [\hat{\boldsymbol{x}}^j_{k|k} - \hat{\boldsymbol{x}}_{k|k}][\hat{\boldsymbol{x}}^j_{k|k} - \hat{\boldsymbol{x}}_{k|k}]^T\} \tag{27b}$$

Algorithm 1 presents a schematic description of one cycle of the IMM algorithm.

Algorithm 1 Generic IMM algorithm

1: Obtain previous step's data $\{\mu^i_{k-1}, \hat{\boldsymbol{x}}^i_{k-1|k-1}, \boldsymbol{P}^i_{k-1|k-1}\}_{i=1}^s$
2: Calculate mixing probabilities $\mu^{i|j}_{k-1}$ via Eq. (22)
3: **for** all $j = 1, \ldots, s$ **do**
4: Calculate jth filter initial conditions $\hat{\boldsymbol{x}}^{0j}_{k-1|k-1}$ [Eq. (23)] and $\boldsymbol{P}^{0j}_{k-1|k-1}$ [Eq. (24)]
5: Perform mode-matched filtering via KF equations (Sec. III.B)
6: **end for**
7: **for** all $j = 1, \ldots, s$ **do**
8: Update mode probabilities μ^j_k [Eq. (26)]
9: **end for**
10: Calculate combined estimation $\hat{\boldsymbol{x}}_{k|k}$ and covariance $\boldsymbol{P}_{k|k}$ via Eqs. (27)

B. Target-Tracking IMM

The target-tracking EKF-based IMM proposed in this paper is based on the generic IMM algorithm presented in the previous subsection, adapted to the models formulated in Sec. II. The problem-specific steps of the algorithm, presented herein, are model-matched filtering and filter initialization.

1. Model-Matched Filtering

As the target model is nonlinear, an EKF model-matched filter is developed. The state estimate of the filter matched to the jth mode at time k using information up to time $k-1$, $\hat{\boldsymbol{x}}^j_{k|k-1}$, is calculated by using Eq. (7) for $r_k = j$.

The Jacobian matrix associated with the dynamics of Eq. (4) is

$$\boldsymbol{F}^j_x = \left[\begin{array}{cccc} 0 & V_{\lambda i} & V_T\sin(\gamma_{t;T}+\lambda_{t;i}) & 0 \\ -V_{\lambda i}/\rho^2_{t;i} & -V_{\rho i}/\rho_{t;i} & V_T\cos(\gamma_{t;T}+\lambda_{t;i})/\rho_{t;i} & 0 \\ 0 & 0 & 0 & 1/V_T \\ 0 & 0 & 0 & -1/\tau_T \end{array}\right]\Bigg|_{\boldsymbol{x}=\hat{\boldsymbol{x}}^{0j}_{k-1|k-1}} \tag{28}$$

Therefore, the prediction error covariance matrix of the filter matched to the jth mode is

$$\boldsymbol{P}^j_{k|k-1} = \boldsymbol{\Phi}_{k,k-1}\boldsymbol{P}^{0j}_{k-1|k-1}\boldsymbol{\Phi}^T_{k,k-1} + \boldsymbol{Q}_d \tag{29}$$

where

$$\boldsymbol{\Phi}_{k,k-1} = e^{\boldsymbol{F}^j_x T} \tag{30}$$

is the transition matrix associated with the system dynamics, assuming that $\boldsymbol{F}^j_x$ is fixed during the interval $(t_{k-1}, t_k]$, $T = t_k - t_{k-1}$ is the sampling time, and $\boldsymbol{Q}_d$ is the covariance matrix of the equivalent discrete process noise, used as a tuning matrix.

The next step is measurement update, which depends on whether information is shared between the missiles or not. We first present the general equations, and then we specify the details of each case.

The updated state estimate of the filter matched to the jth model is

$$\hat{\boldsymbol{x}}^j_{k|k} = \hat{\boldsymbol{x}}^j_{k|k-1} + \boldsymbol{K}^j_k[z_k - \boldsymbol{h}_k(\hat{\boldsymbol{x}}^j_{k|k-1})] \tag{31}$$

where $\boldsymbol{K}^j_k$ is the Kalman gain, computed as

$$\boldsymbol{K}^j_k = \boldsymbol{P}^j_{k|k-1}[\boldsymbol{H}^j_x]^T[\boldsymbol{S}^j_k]^{-1} \tag{32a}$$

$$\boldsymbol{S}^j_k = \boldsymbol{H}^j_x\boldsymbol{P}^j_{k|k-1}[\boldsymbol{H}^j_x]^T + \boldsymbol{R} \tag{32b}$$

$\boldsymbol{S}^j_k$ is the covariance of the innovations process, $\boldsymbol{R}$ is the measurement noise covariance matrix, and $\boldsymbol{H}^j_x$ is the measurement Jacobian matrix:

$$\boldsymbol{H}^j_x(l, p) = \left.\frac{\partial h_l}{\partial x_p}\right|_{\boldsymbol{x}=\hat{\boldsymbol{x}}^j_{k|k-1}} \tag{33}$$

The updated covariance matrix is calculated using the Joseph formula:

$$\boldsymbol{P}^j_{k|k} = [\boldsymbol{I} - \boldsymbol{K}^j_k\boldsymbol{H}^j_x]\boldsymbol{P}^j_{k|k-1}[\boldsymbol{I} - \boldsymbol{K}^j_k\boldsymbol{H}^j_x]^T + \boldsymbol{K}^j_k\boldsymbol{R}[\boldsymbol{K}^j_k]^T \tag{34}$$

and the mode conditioned likelihood Λ^j_k is calculated using the innovations process distribution:

$$\Lambda^j_k = p(z_k|r_k = j, \mathcal{Z}_{k-1}) \sim \mathcal{N}(z_k; \hat{z}^j_{k|k-1}, \boldsymbol{S}^j_k) \tag{35}$$

where $\hat{z}^j_{k|k-1}$ is the predicted measurement (computed by the filter).

When the estimation is performed by the ith missile using own-missile measurements only (information nonsharing mode), the measurement Jacobian matrix [derived from Eq. (9)] and the measurement noise covariance matrix are

$$\boldsymbol{H}^j_x = [0 \quad -1 \quad 0 \quad 0]|_{\boldsymbol{x}=\hat{\boldsymbol{x}}^j_{k|k-1}}, \qquad \boldsymbol{R} = [\sigma^2_i] \tag{36}$$

For the case where the estimation is performed using measurements from multiple missiles (information-sharing mode), the measurement Jacobian matrix of the ith missile [derived from Eq. (11)] and the measurement noise covariance matrix are

$$\boldsymbol{H}^j_x = \left[\begin{array}{cccc} [\boldsymbol{H}^j_x]_{1,1} & [\boldsymbol{H}^j_x]_{1,2} & 0 & 0 \\ [\boldsymbol{H}^j_x]_{2,1} & [\boldsymbol{H}^j_x]_{2,2} & 0 & 0 \\ \vdots & \vdots & \vdots & \vdots \\ [\boldsymbol{H}^j_x]_{m,1} & [\boldsymbol{H}^j_x]_{m,2} & 0 & 0 \end{array}\right]\Bigg|_{\boldsymbol{x}=\hat{\boldsymbol{x}}^j_{k|k-1}}, \quad \boldsymbol{R} = \mathrm{diag}\{\sigma^2_1, \sigma^2_2, \ldots, \sigma^2_m\} \tag{37}$$

where

$$[\boldsymbol{H}_x^j]_{l,1} = \frac{\Delta Y_{il}\cos(\lambda_{k;i}) - \Delta X_{il}\sin(\lambda_{k;i})}{\Delta R_{il}^2 + \rho_{k;i}^2 + 2\rho_{k;i}[\Delta X_{il}\cos(\lambda_{k;i}) + \Delta Y_{il}\sin(\lambda_{k;i})]} \tag{38a}$$

$$[\boldsymbol{H}_x^j]_{l,2} = -\frac{[\Delta X_{il}\cos(\lambda_{k;i}) + \Delta Y_{il}\sin(\lambda_{k;i}) + \rho_{k;i}]\rho_{k;i}}{\Delta R_{il}^2 + \rho_{k;i}^2 + 2\rho_{k;i}[\Delta X_{il}\cos(\lambda_{k;i}) + \Delta Y_{il}\sin(\lambda_{k;i})]} \tag{38b}$$

and

$$\Delta X_{il} \triangleq x_{k;i} - x_{k;l}; \quad \Delta Y_{il} \triangleq y_{k;i} - y_{k;l}; \quad \Delta R_{il} \triangleq (\Delta X_{il}^2 + \Delta Y_{il}^2)^{1/2} \tag{39}$$

for $l \in \{1, 2, \ldots, m\}$. The ith missile's relative states $\rho_{k;i}$ and $\lambda_{k;i}$ in Eqs. (38) are substituted with the appropriate values from the estimated state vector $\hat{\boldsymbol{x}}_{k|k-1}^j$; and the positions of the missiles $x_{k;i}$, $x_{k;l}$, $y_{k;i}$, and $y_{k;l}$ are taken in the kth time frame.

2. *Filter Initialization*

The IMM requires Gaussian initial conditions. Although the initializing radar's measurement is Gaussian [Eq. (15)], the transformation of these initial conditions to the ith missile's relative state vector renders it no longer Gaussian because the geometric relation between the radar's state and the ith missile's relative state vector is nonlinear [Eqs. (16)]. We therefore linearize Eqs. (16) about the expected value $\bar{\boldsymbol{x}}_{0;R}$ to obtain approximate Gaussian initial conditions for the proposed filter. The ith missile's initial conditions

$$\hat{\boldsymbol{x}}_{0|0} \sim \mathcal{N}(\bar{\boldsymbol{x}}_0, \boldsymbol{P}_0) \tag{40}$$

are calculated as follows. The expected value $\bar{\boldsymbol{x}}_0$ is derived by substituting the expected value of the radar state $\bar{\boldsymbol{x}}_{0;R}$ in Eqs. (16). Note that $\gamma_{0;T}$ and $a_{0;T}$ are given directly. The covariance matrix $\boldsymbol{P}_0$ is derived by applying the following transformation:

$$\boldsymbol{P}_0 = \boldsymbol{G}\boldsymbol{P}_{0;R}\boldsymbol{G}^T; \qquad \boldsymbol{G} = \begin{bmatrix} \boldsymbol{G}_x & [\boldsymbol{0}]_{2\times 2} \\ [\boldsymbol{0}]_{2\times 2} & \boldsymbol{I}_{2\times 2} \end{bmatrix} \tag{41}$$

with $[\boldsymbol{0}]$ and $\boldsymbol{I}$ denoting a matrix of zeros and the identity matrix, respectively. $\boldsymbol{G}_x$ is the Jacobian matrix associated with Eq. (16):

$$\boldsymbol{G}_x = \left.\begin{bmatrix} [\boldsymbol{G}_x]_{1,1} & [\boldsymbol{G}_x]_{1,2} \\ [\boldsymbol{G}_x]_{2,1} & [\boldsymbol{G}_x]_{2,2} \end{bmatrix}\right|_{\boldsymbol{x}_{0;R}=\bar{\boldsymbol{x}}_{0;R}} \tag{42}$$

where

$$[\boldsymbol{G}_x]_{1,1} = \frac{\rho_{0;R} + \Delta X_{Ri}\cos(\lambda_{0;R}) + \Delta Y_{Ri}\sin(\lambda_{0;R})}{\rho_{0;i}} \tag{43a}$$

$$[\boldsymbol{G}_x]_{1,2} = \frac{\rho_{0;R}[\Delta Y_{Ri}\cos(\lambda_{0;R}) - \Delta X_{Ri}\sin(\lambda_{0;R})]}{\rho_{0;i}} \tag{43b}$$

$$[\boldsymbol{G}_x]_{2,1} = \frac{\Delta X_{Ri}\sin(\lambda_{0;R}) - \Delta Y_{Ri}\cos(\lambda_{0;R})}{\rho_{0;i}^2} \tag{43c}$$

$$[\boldsymbol{G}_x]_{2,2} = \frac{\rho_{0;R}^2 + \rho_{0;R}[\Delta X_{Ri}\cos(\lambda_{0;R}) + \Delta Y_{Ri}\sin(\lambda_{0;R})]}{\rho_{0;i}^2} \tag{43d}$$

$\rho_{0;i}$ is calculated via Eq. (16a), and ΔX_{Ri} and ΔY_{Ri} are calculated via Eqs. (17).

IV. Guidance and Missile Staggering Strategy

In this section, we present the missile guidance laws and the derivation of the missile staggering strategy. For simplicity, we limit the discussion to two intercepting missiles, but a similar methodology can also be applied to larger interception teams. We derive the staggering strategy based on a linearized model. Our main motivation for using the linearized model is the BMD scenario that occurs at very high interception speeds in which the linearization assumption holds very well.

A. Perfect Information Missile Guidance Laws

Two types of guidance laws are used in this paper, which are derived based on different perfect information formulations and assumptions on the linear model: linear quadratic guidance laws (LQGLs) and bounded control guidance laws (BCGLs). LQGLs can be derived based on a linear-quadratic optimal control or differential game formulation, with different assumptions on the missile and target dynamics, and have the following general structure for the ith missile:

$$u_{t;i} = \frac{N_j Z_j}{t_{\text{go};i}^2\cos(\delta_{0;i})}, \qquad j \in \{\text{PN}, \text{APN}, \text{OGL}, \text{LQDG}\} \tag{44}$$

where Z_j is the zero-effort miss (ZEM), which is specific for each guidance law:

$$Z_{\text{PN}} = \xi_{t;i} + \dot{\xi}_{t;i} t_{\text{go};i} \tag{45a}$$

$$Z_{\text{APN}} = Z_{\text{PN}} + a_{t;Ti}^{n0} t_{\text{go};i}^2/2 \tag{45b}$$

$$Z_{\text{OGL}} = Z_{\text{PN}} + a_{t;Ti}^{n0} t_{\text{go};i}^2/2 - a_{t;i}^{n0}\tau_i^2\psi(\theta) \tag{45c}$$

$$Z_{\text{LQDG}} = Z_{\text{PN}} + a_{t;Ti}^{n0}\tau_T^2\psi(\theta/\varepsilon) - a_{t;i}^{n0}\tau_i^2\psi(\theta) \tag{45d}$$

N_j is the navigation gain, which is constant for PN and APN, but is time dependent for OGL and LQDG. The time-dependent navigation gains of OGL and LQDG are given by

$$N_{\text{OGL}} = \frac{6\theta^2\psi(\theta)}{\Delta(\theta)}, \qquad \Delta(\theta) = 3 + 6\theta - 6\theta^2 + 2\theta^3 - 3e^{-2\theta} - 12\theta e^{-\theta} + 6/(b\tau_i^3) \tag{46a}$$

$$N_{\text{LQDG}} = \frac{6\theta^2\psi(\theta)}{\Delta(\theta) + \gamma^{-2} f(\theta, \theta/\varepsilon)}, \qquad f(\theta, \theta/\varepsilon) = -3\varepsilon^3 - 6\varepsilon^2\theta + 6\varepsilon\theta^2 + 12\varepsilon^2\theta e^{-\theta/\varepsilon} + 3\varepsilon^3 e^{-2\theta/\varepsilon} \tag{46b}$$

where b and γ are the weights on the miss distance and the target control effort, respectively, in the quadratic cost functions [4]. The ith missile's time to go $t_{\text{go};i}$ is given for the linear model by

$$t_{\text{go};i} = \frac{\rho_{t;i}}{V_c}, \qquad V_c = V_{t;i}\cos(\delta_{0;i}) + V_{t;T}\cos(\delta_{0;Ti}) \tag{47}$$

and θ, ε, and $\psi(\eta)$ are given by

$$\theta = t_{go;i}/\tau_i, \qquad \varepsilon = \tau_T/\tau_i, \qquad \psi(\eta) = e^{-\eta} + \eta - 1 \tag{48}$$

The BCGLs can be derived by formulating a bounded control differential game and have generally two types of structures. The bang–bang structure is

$$u_{t;i} = a_i^{\max}\text{sign}[Z_j], \qquad j \in \{\text{DGL0}, \text{DGL1}\} \tag{49}$$

where $a_i^{\max}$ is the maximal missile acceleration command. In the saturated linear structure, the command is linear in part of the singular region, until the saturation value is reached, and a bang–bang command is applied outside the singular region:

$$u_{t;i} = \begin{cases} a_i^{\max}\text{sat}[Z_j/(kZ^*)] & \text{in the singular region} \\ a_i^{\max}\text{sign}[Z_j] & \text{else} \end{cases}, \quad j \in \{\text{DGL0}, \text{DGL1}\} \tag{50}$$

where "sign" and "sat" are the signum and saturation functions, respectively; $0 < k \leq 1$ is the portion of the singular region in which the acceleration is linear; Z_j is the ZEM of each guidance law

$$Z_{\text{DGL0}} = Z_{\text{PN}} - a_{t;i}^{n0}\tau_i^2\psi(\theta) \tag{51a}$$

$$Z_{\text{DGL1}} = Z_{\text{PN}} + a_{t;Ti}^{n0}\tau_T^2\psi(\theta/\varepsilon) - a_{t;i}^{n0}\tau_i^2\psi(\theta) \tag{51b}$$

and Z^* is the boundary of the singular region. The logic behind the choice in Eq. (50) is that the optimal command in the singular region is arbitrary; thus, a linear command can be used to prevent chattering. A detailed description of the DGL0 and DGL1 laws can be found in [5,6], respectively.

B. Estimation Process Model

The perfect information performance of any perfect information guidance law (and, in particular, the guidance laws of Sec. IV.A) is substantially better than the performance of the same guidance law using estimated states. Thus, if the guidance law is given, like in the case at hand, a logical approach for improving the interception performance is to model the estimation error, use this model to understand how the estimation error induces miss, and use this insight to reduce the estimation error or to compensate for it in some appropriate manner.

The estimation process is stochastic and, due to the non-Gaussian nature of the target maneuver and the nonlinear kinematics, it is not necessarily Gaussian. We would like to approximate this process by a deterministic model, which will capture its main effects on the closed-loop interception performance. It is well known [14] that the most dominant estimation error in modern guidance laws that use target acceleration (like OGL, LQDG, and DGL1) is related to the estimation of the target acceleration. The estimation of the target acceleration is typically time delayed, mainly because it is based on the bearing measurement. A simple physical relation, which is independent of the estimator, for predicting this time delay was originally suggested in [24]. The target acceleration manifests in the bearing measurement only after the target displacement perpendicular to the LOS is significant relative to the sensor noise. From Eq. (20), it is clear that, once a target acceleration command is initiated, it has to pass through a low-pass filter, due to the target dynamics, and then be integrated twice before a displacement perpendicular to the LOS is generated. This third-order system is the cause for the delay between the actual mode change of the target and the identification of the mode change by the estimator.

The time response of this third-order system to a step target acceleration command can be approximated, for short time intervals, by

$$\Delta\xi \approx \frac{\Delta u_T t^3}{6\tau_T} \tag{52}$$

where $\Delta\xi$ and Δu_T are the relative displacement perpendicular to the LOS and the acceleration command change, respectively. Rearranging Eq. (52) and requiring that the target deviates two standard deviations from the estimate, $\Delta\xi = 2\sigma_{\dot{\xi}}$ (so that it can be identified by the estimator) yields the following time delay in the estimator's mode change identification

$$\tau_r \approx \left(\frac{12\tau_T\sigma_{\dot{\xi}}}{\Delta u_T}\right)^{1/3} \tag{53}$$

Assuming small deviations from the collision triangle, the displacement $\xi_{t;i}$ normal to the ith initial LOS can be approximated by

$$\xi_{t;i} \approx (\lambda_{t;i} - \lambda_{0;i})\rho_{t;i} \tag{54}$$

Thus, if we assume that the estimation error of $\rho_{t;i}$ is small, which is the case at ranges for which the target evasive maneuvers are effective, we can approximate $\sigma_{\dot{\xi}}$ by $\sigma_{\dot{\xi}} \approx \rho_{t;i}\sigma_\lambda$, where σ_λ is the standard deviation of the bearing measurement. Substituting this approximation into Eq. (53) yields

$$\tau_r \approx \left(\frac{12\tau_T\rho_{t;i}\sigma_\lambda}{\Delta u_T}\right)^{1/3} \tag{55}$$

Since the target acceleration error induces a dominant part of the miss distance [14], we model the estimation process as perfect information with a pure target acceleration delay, where the delay is given by Eq. (55):

$$\hat{\mathbf{y}}_{t;i} = [\,\xi_{t;i} \quad \dot{\xi}_{t;i} \quad a_{t;i} \quad a_{t-\tau_r;T}\,]^T \tag{56}$$

Because the target estimation delay is the only effect in the model of the estimation process, and because the delay is smaller at closer ranges, we model the information-sharing mode by passing the leading missile's target acceleration to the trailing missile. After the leading missile intercepts the target, its estimate no longer exists and the trailing missile's estimation of the target's acceleration is based on its own range to the target.

Notice that, in Eq. (55), the time delay of the target mode change identification depends in the same manner on the range $\rho_{t;i}$ and on the sensor quality σ_λ. Thus, if we stagger the launch of the missiles and share information between them, the leading missile will act as an improved sensor for the trailing missile. In the proposed estimation process model, this is the main estimation benefit from information sharing.

C. Missile Staggering Strategy

We use a linear deterministic simulation to obtain a better understanding of the effects of the target estimation time delay and information sharing on the interception performance. The simulation combines the linear model of Sec. II.D, the guidance laws of Sec. IV. A, and the estimation process model of Sec. IV.B. We will then use this understanding to derive the missile launch staggering strategy.

1. *Linear Simulation Scenario*

The simulation is performed in a BMD scenario and includes two intercepting missiles and a single target. The engagements are initiated at a separation of 15,000 m between the leading missile and the target, with the trailing missile at different trailing distances behind the leading missile. The missiles and target are initiated at a head-on geometry. The target speed is $V_T = 2500$ m/s and its maneuver capability is $a_T^{\max} = 20$ g. The missile and target first-order time constants are $\tau_i = 0.2$ s and $\tau_T = 0.2$ s, respectively. Both missiles fly at a constant speed of $V_i = 2500$ m/s, their maximal maneuver capability is $a_i^{\max} = 45$ g, the standard deviations of their IR sensors are $\sigma_i = 0.5$ mrad, and they use DGL1 with a linear command in the singular region and $k = 0.7$.

We assume that, in order to evade capture, the target performs a bang–bang maximal acceleration maneuver, which is the optimal

maneuver structure with a bounded acceleration command. As a first step, we assume a single target direction switch during the engagement. The rationale behind this choice is the short engagement time and the assumption that the target is not aware of the missiles' position and chooses its maneuver time randomly. This seems a reasonable assumption that is typically used in such scenarios [11,14]. However, as we show in the sequel, when the missiles are staggered, an intelligent target can perform two acceleration switches: one to evade each interceptor. To be conservative, we therefore modify the staggering strategy to cope with this possible target strategy.

2. *Single Target Switch*

Figure 4 presents the miss distance as a function of the target switch time for both missiles in the information-sharing (solid line) and nonsharing (dashed line) modes, with different selections of the staggering distance between the missiles ΔX. (See online version of paper for color versions of Fig. 4 and all figures thereafter.) The leading missile (missile 1) is not affected by the information sharing in our deterministic estimation model; thus, only one curve is presented for each staggering distance. The team's miss at each target switch time is the minimum value between the curves of the leading missile and the trailing missile. In the same scenario with perfect information, DGL1 can guarantee zero miss, because the maneuver ratio satisfies $\mu = a_i^{\max}/a_T^{\max} > 1$ and the agility satisfies $\mu\varepsilon > 1$. The miss is therefore a result of the estimation model (i.e., estimation delay of the target acceleration) and is generated as follows. The missiles are initially unaware of the target acceleration switch, due to their estimation delay, which results in a ZEM error. When the missiles become aware of the target acceleration switch, they can no longer correct it due their bounded acceleration command and the time left until interception. When the target switches too early, the time left until the end of the engagement allows the missiles to correct the ZEM error. This explains the zero miss of missile 1 for switch times smaller than 2 s in Fig. 4. When the target switches too late, it does not have sufficient time to generate a ZEM error, due to its own bounded acceleration and dynamics. This explains the smaller-than-maximum miss distances of missile 1 when the target switches after 2.3 s.

It is evident from Fig. 4 that the team miss distance (in both the sharing and nonsharing modes) decreases as the staggering between the missiles increases. This is because, to induce a miss, the target has to maneuver in a time window of approximately 1 s before interception (in this scenario), and the maximum miss is induced when the target maneuvers at approximately 0.7 s before interception. Thus, if the target switches only once, and the maneuver windows of the missiles do not overlap, the team performance improves even without information sharing. Note that this effect stems merely from the cooperation in guidance (by staggering). The staggering distance to exploit this effect depends on the guidance laws used by the missiles, the players' dynamic parameters, maneuver capability, and sensor quality. To fully exploit this effect, in the case at hand and without information sharing, the missile intercepts need to be staggered by more than $\Delta T_{\text{int}} = 1$ s. For a closing speed of $V_c = V_2 + V_T = 5000$ m/s, this time separation is equivalent to more than $\Delta X = V_c \Delta T_{\text{int}} = 5000$ m, or a launch staggering of $\Delta T_l = \Delta X/V_1 = 2$ s. The main limitation of relying on this effect only, as we demonstrate in the sequel, is that staggering the missiles too far from each other permits the target to perform two acceleration switches: one against each missile.

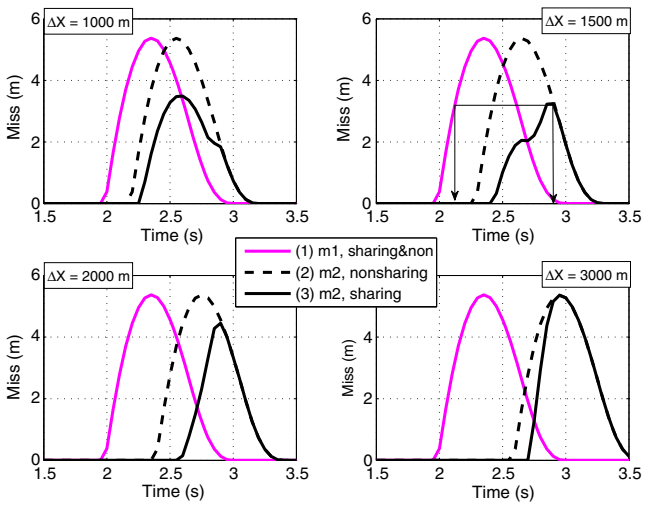

Fig. 4 Miss distance, linear simulation, DGL1, and $\Delta X = 1000$–3000 m: missile 1 information-sharing and nonsharing modes (line 1); missile 2 information-nonsharing mode (line 2); and missile 2 information-sharing mode (line 3).

It is also evident from Fig. 4 that information sharing reduces the miss distance of missile 2 (trailing missile), which leads to a further improvement of the team performance at the same staggering distance. This improvement is a result of the smaller target estimation time delay, which is available to the trailing missile from the closer leading missile. The improvement is only available if the target maneuvers before the leading missile passes the target or, more precisely, until one sample before interception (or blind zone) minus the leading missile's own time delay at that sample. We refer to this time as the last information time (LIT). This explains the performance convergence of missile 2 in the sharing and nonsharing modes shortly before missile 1 intercepts the target, at $t = 3$ s. Thus, if the missiles are staggered such that the maximal miss distance of the trailing missile occurs after the LIT, its maximal miss is not improved by information sharing. However, the team performance might still slightly improve, due to miss reduction in the effective maneuver window before the maximal miss, like in the $\Delta X = 3000$ m case in Fig. 4. We have demonstrated that, in the information-sharing mode, performance at the same staggering distance for overlapping effective interception windows is better than without information sharing. The main advantage of information sharing is that the team performance substantially improves even at relative small staggering distances, for which employing a two-switch evasive maneuver does not benefit the target because the proximity of the two switches reduces their effectiveness.

3. *Two Target Switches*

Our staggering strategy for the information-sharing case is based on a conservative assumption that the target might also perform a two-switch maneuver. Based on the previous analysis, we propose to choose the missile staggering such that the intersection between the miss curves is slightly lower than the miss value of the trailing missile at the LIT, which in our case would be around $\Delta X = 1500$ m. The rationale behind this choice is that, for a single target switch, this guarantees the team at least the miss value at the curve intersection, which is less than the value of the trailing missile at the LIT point. Furthermore, if the target performs two switches, with the first switch to evade the leading missile, this will only reduce the trailing missile's miss distance at the LIT point, as this will generate less initial ZEM error that the trailing missile would have to correct.

With the proposed missile staggering strategy, we expect the optimal two-switch target maneuver to be a first switch against missile 1 at approximately the time when the left part of its miss curve (at switch times lower than the maximal miss) has the same miss value as missile 2 at the LIT, as well as a second switch at the LIT (marked on the $\Delta X = 1500$ m subplot of Fig. 4). This will minimize the effect of the first switch on missile 2 and result in at least the same miss for missile 1 because the second switch will be close to its interception. Thus, the team miss for a two-switch maneuver will be upper-bounded by the miss at the LIT. Any other target two-switch selection will result in a lower team miss.

Figure 5 presents the team miss distance for any two-switch target maneuver for the $\Delta X = 1500$ m case, which confirms our prediction regarding the optimal target evasion strategy and the maximal guaranteed miss distance of about 3 m. We can also see that, for a single switch, we get a lower miss of about 2 m for a switch at $t \approx 2.7$ s. Note that we do not choose the miss at the curve intersection and the LIT to be exactly the same because it will practically be very hard, even for an intelligent target with perfect information, to

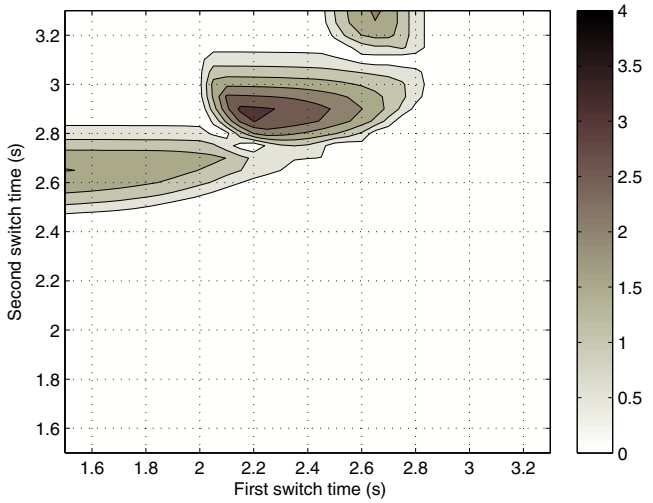

Fig. 5 Team miss distance, linear simulation, two-switch target maneuver, DGL1, and $\Delta X = 1500$ m. The shades indicate the team miss distances for different combinations of target switch times.

exactly perform the optimal two-switch maneuver, which will reduce the maximal two-switch miss even more.

Figure 6 presents the team miss distance for any two-switch target maneuver for a missile staggering of $\Delta X = 2000$ m, for comparison. It is evident that, although the single-switch target maneuver is slightly better in this case, with a miss of about 1.6 m compared with a miss of about 2 m, the two-switch target maneuver is much worse, with a miss of about 4 m compared to a miss of about 3 m. This clarifies why staggering the missiles even more will guarantee the missiles' team even worse performance.

V. Design Considerations and Implementation Issues

Implementing the guidance laws of Eqs. (44), (49), and (50) in a nonlinear setting is performed as follows. Using the assumption of small deviations from the collision triangle, differentiating Eq. (54) with respect to time, and substituting in Eq. (45a) yields

$$Z_{\mathrm{PN}} = \xi_{t;i} + \dot{\xi}_{t;i} t_{\mathrm{go};i} = -V_{\rho i} t_{\mathrm{go};i}^2 \dot{\lambda}_{t;i} \tag{57}$$

Using this expression for the computation of each ZEM in Eqs. (45) and (50) replaces the dependence on $\xi_{t;i}$, $\dot{\xi}_{t;i}$ by $\dot{\lambda}_{t;i}$ and $V_{\rho i}$, which can be calculated via the nonlinear dynamics in Eqs. (4) and (5). Due to the same assumption, $t_{\mathrm{go};i}$ can be approximated by

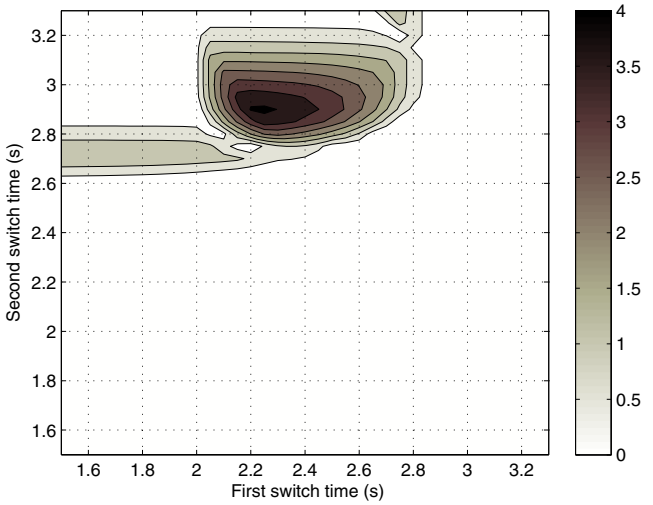

Fig. 6 Team miss distance, linear simulation, two-switch target maneuver, DGL1, and $\Delta X = 2000$ m. The shades indicate the team miss distances for different combinations of target switch times.

$$t_{\mathrm{go};i} \approx -\frac{\rho_{t;i}}{V_{\rho i}} \tag{58}$$

The final adjustment to the nonlinear setting is to perform all the calculations relative to the instantaneous LOS and not with respect to the initial LOS. Thus, Eq. (44) is replaced by

$$u_{t;i} = \frac{N_j Z_j}{t_{\mathrm{go};i}^2 \cos(\delta_{t;i})}, \qquad j \in \{\mathrm{PN}, \mathrm{APN}, \mathrm{OGL}, \mathrm{LQDG}\} \tag{59}$$

and the accelerations normal to the initial LOS, $a_{t;Ti}^{n0}$, and $a_{t;i}^{n0}$ in Eqs. (45) and (51) are replaced by the acceleration normal to the instantaneous LOS:

$$a_{t;Ti}^{n} = a_{t;T} \cos(\delta_{t;Ti}), \qquad a_{t;i}^{n} = a_{t;i} \cos(\delta_{t;i}) \tag{60}$$

Determining the missiles' staggering can be done in two ways. Assuming that the target is identified by the tracking radar before the missiles are launched, one can either run a deterministic simulation in real time, which needs to be completed before the second missile is launched, or pull the staggering time from a precalculated look up table for different target parameters like $a_T^{\max}$, V_T, τ_T, and $\gamma_{t;T}$. In BMD scenarios, the initial target's flight-path angle $\gamma_{t;T}$ and speed V_T are determined largely by the location the target (incoming missile) is launched from; and $a_T^{\max}$ and τ_T are typically functions of the incoming target's design and the planned intercept altitude. Thus, because we assume that the target is identified, intelligence on the target is available and, to reduce any noncritical calculations before launch, producing lookup tables for different threats is feasible. However, real-time calculation can also be performed, as it can be easily parallelized because it is built up of multiple single-run deterministic simulations. Note that only switch times within the effective target evasion window (in this case, of approximately the last second before intercept) need to be considered. Furthermore, because the maximal miss of the second missile needs to occur before the LIT, only staggering of approximately half of the effective window needs to be considered, which also reduces the number of simulations considerably.

The information-sharing concept relies on continuous communication between the intercepting missiles. Information delays can be corrected by using a time stamp on the information and propagation of the filter to the correct time before measurement update. However, delays occurring very close to the leading missile's intercept can lead to an increase in the delay of the target acceleration estimation, and even to loss of information, which cannot be corrected if the leading missile's proximity fuse is initiated before the information is passed. Therefore, minimal communication delay is especially important just before the leading missile intercepts the target, as this is the time when information of the highest quality is transmitted to the trailing missile. It is expected that, if the communication delays at that time are similar in size to the expected improvement in the estimation delay of target acceleration at the critical target maneuver time (i.e., approximately 0.05 s according to the simulations presented in Sec. VI.B), then the main benefit of information sharing would be substantially smaller. These arguments, as well as the fact that the missiles are substantially closer to one another than to the ground radar or launch center, suggest a missile-to-missile communication architecture.

In the proposed staggering strategy, the missiles are launched one after the other, which leads to very similar trajectories. Basically, the trailing missile follows the leading missile. Thus, to reduce sensitivity to jamming, directional communication is recommended. High gain antennas, with a narrow field of view, can be positioned at the front and aft parts of the missiles. Thus, the leading missile can transmit/receive directly backward and the trailing missile can transmit/receive directly forward. This type of communication renders jamming substantially more difficult and requires substantially less transmission power. It should be noted that information from the leading missile to the trailing missile is substantially more important than the information from the trailing missile to the leading missile.

In passing, we note that, although focusing on the novel idea of engagement staggering and information sharing, we have avoided addressing a number of real-life implementation issues, such as alignment errors between the missiles' frames of reference (such errors are handled, in multiagent systems, in a variety of ways and means). Addressing these issues, which is deemed outside the scope of the present paper, will need to be done before the new concept is implemented in a real-life system.

VI. Simulation Study

The performance of the cooperative estimator and the missile staggering strategy developed in this paper are evaluated in this section via simulation, using nonlinear kinematics and the missile and target dynamics. We first present the simulation environment and interception scenario. We then analyze the estimation performance in open loop and compare its performance in the information-sharing and nonsharing configurations. We then evaluate the information-sharing effect on the guidance accuracy in closed loop via a Monte Carlo (MC) simulation.

A. Simulation Environment and Scenario

The simulation is performed in a BMD scenario and includes two intercepting missiles and a single target. The engagements are initiated at a vertical separation of 15,000 m between the leading missile and the target, with the trailing missile at different trailing distances behind the leading missile. The missiles and target are initiated at head-on geometry, with the missiles at a 50 m horizontal separation on both sides of the target. The target is initialized in the $-Y_I$ direction with a flight-path angle of $\gamma_{0;T} = -\pi/2$ rad. The missiles' flight-path angles are chosen such that the missiles velocity vectors point toward the initial target location. The target speed is $V_T = 2500$ m/s, its maneuver capability is $a_T^{\max} = 20$ g, and it performs a bang–bang maximal acceleration maneuver with a single direction switch during the engagement. The missiles' and target's first-order time constants are $\tau_i = 0.2$ s and $\tau_T = 0.2$ s, respectively. Both missiles fly at a constant speed of $V_i = 2500$ m/s, and their maximal maneuver capability is $a_i^{\max} = 45$ g; the standard deviation of their IR sensor is $\sigma_i = 0.5$ mrad, and they use the DGL1 guidance law with a linear command in the singular region and $k = 0.7$ (when not stated otherwise).

The states needed for the guidance laws' employment are estimated at each time step, using the estimator derived in Sec. III, at a sampling rate of 100 Hz. For evaluating the estimation performance in open loop (Sec. VI.B), perfect information (true state vector) is used to guide the missiles; whereas when evaluating the closed-loop interception performance (Sec. VI.C), the estimated state from the estimator is used to guide the missiles. When running the estimation in the information-sharing mode, the leading missile's measurements are used only if the missile is still active. A missile is considered active if $\rho_{k+1;i} < \rho_{k;i}$.

The initial radar's estimate is chosen to satisfy

$$\hat{\boldsymbol{x}}_{0;R} \sim \mathcal{N}(\bar{\boldsymbol{x}}_{0;R}, \boldsymbol{P}_{0;R}) \tag{61}$$

where $\bar{\boldsymbol{x}}_{0;R}$ is the true target initial state, and

$$\boldsymbol{P}_{0;R} = \text{diag}\left\{50^2, (1\pi/180)^2, (3\pi/180)^2, 10^2\right\} \tag{62}$$

The initial mode probabilities are chosen to be equal for both possible modes, and the transition probability matrix is chosen to be

$$\Pi = \begin{bmatrix} 0.99 & 0.01 \\ 0.01 & 0.99 \end{bmatrix} \tag{63}$$

The comparison between the sharing and nonsharing modes is performed using the same random noises and initial conditions. The equations of motion of the missiles and the target are solved using a fourth-order Runge–Kutta algorithm. To ensure precise miss distance evaluation, high-resolution integration is performed when the missile is at a range of $\rho_{k;i} < 4T(V_T + V_i)$. After the leading missile passes the target, the simulation continues to be run in order to enable evaluation of the trailing missile's performance. We assume that the leading missile does not eliminate the target, even if it passes very close to it, and the team's interception performance is characterized by the smallest of the miss distances of both missiles.

B. Estimator Evaluation and Comparison

To evaluate the statistical characteristics of the estimator, a 200-run Monte Carlo simulation study is performed. Each run uses different random initial conditions and measurement noises, with the same target maneuver (same initial mode and a switch time of 2.5 s). Figures 7 and 8 present the mean and the standard deviation of the estimation error of all the estimated states in sharing and nonsharing modes for a staggering of $\Delta X = 1500$ m. As we expect the main contribution of the sharing mode to be an improvement of the estimation performance of the trailing missile, we concentrate on the trailing missile's performance.

Clearly, the estimation error in range ($\rho_{t;2}$ Err.) in the sharing mode is smaller than in the nonsharing mode. This can be especially seen in the standard deviation, which decreases in time in the sharing mode, unlike its behavior in the nonsharing mode. The reason for this improvement is that, although the horizontal separation between the missiles is only 100 m relative to the 15,000 m initial distance, measurements from two angles are acquired in the sharing mode, which are used to infer on range, unlike in the nonsharing mode. Nevertheless, although this is an obvious improvement, it does not play a major role in the interception performance. The standard deviation in both modes is less than 50 m. Comparing this error to the range at which the optimal target evasive maneuver against missile 2 is performed, at $t = 2.7$ s [which is approximately $(3.3 - 2.7)V_c = 3000$ m], it is evident that the relative range error at which the target maneuver is most effective is approximately 1.5%. This renders the effect of this error negligible and, accordingly, the improvement of the interception performance. The negligible effect of the range error was also confirmed via Monte Carlo simulations by comparing the interception performance obtained when using estimated vs perfect information range information in the guidance loop. This observation is also the main reason for the fact that we do not propose adding a larger horizontal separation between the missiles, in addition to the engagement staggering. The only effect of the horizontal separation will be to improve the observability in range; however, the improvement in range will not lead to substantial improvement in interception performance.

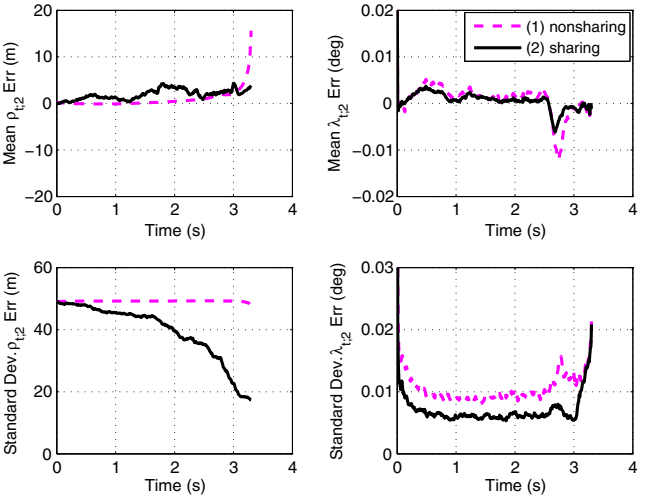

Fig. 7 Range ($\rho_{t;2}$ Err.) and LOS angle ($\lambda_{t;2}$ Err.) estimation errors, nonlinear MC simulation, missile 2, DGL1, and $\Delta X = 1500$ m: information-nonsharing mode (line 1); and information-sharing mode (line 2).

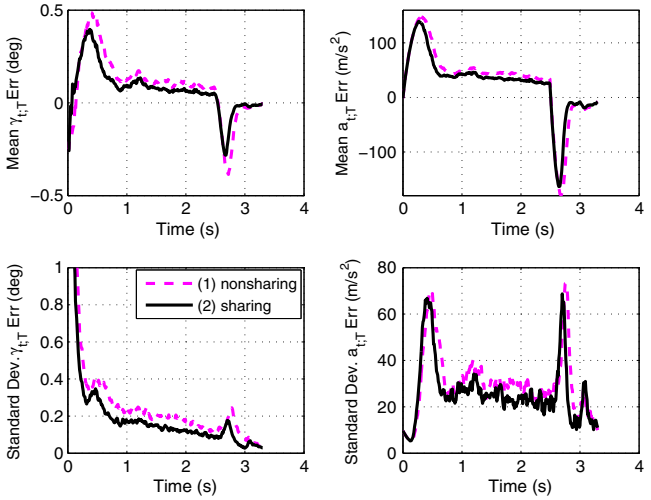

Fig. 8 Flight-path angle ($\gamma_{t;T}$ Err.) and target acceleration estimation ($a_{t;T}$ Err.) errors, nonlinear MC simulation, missile 2, DGL1, $\Delta X = 1500$ m: information-nonsharing mode (line 1); and information-sharing mode (line 2).

The estimation error of the LOS angle ($\lambda_{t;2}$ Err.), in the sharing mode, is also smaller than in the nonsharing mode. This can be seen in both the standard deviation and in the bias after the target maneuver. This improvement is due to the higher-quality measurement acquired by the closer missile (missile 1) and because more measurements are available in the sharing mode. Note that the standard deviation in the sharing mode converges to that of the nonsharing mode at $t \approx 3$ s. This happens because the leading missile's measurement is no longer available after it intercepts the target.

The estimation error of the target flight-path angle ($\gamma_{t;T}$ Err.) and acceleration ($a_{t;T}$ Err.) also improve in both bias and standard deviation. However, the main contributor to the interception performance is the substantially reduced delay in $a_{t;T}$ and the smaller error in $\gamma_{t;T}$ just after the target switch. These effects are harder to observe in Fig. 8, due to their short duration. Note that the target estimation delay is the main contributor we model in the deterministic estimation model. Thus, it is expected to improve before the deterministic model can be used for planning the missile staggering.

Figure 9 compares the estimated target acceleration $a_{t;T}$ of both missiles in the sharing and nonsharing modes. The figure also presents the true target acceleration and the pure delayed target

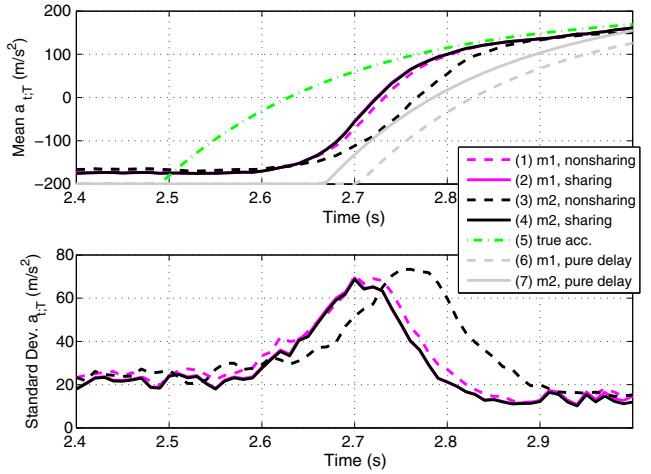

Fig. 9 Target acceleration estimation ($a_{t;T}$) at the switch ($t_{sw} = 2.5$ s), nonlinear MC simulation, both missiles, DGL1, and $\Delta X = 1500$ m: missile 1, information-nonsharing mode (line 1); missile 1, information-sharing mode (line 2); missile 2, information-nonsharing mode (line 3); missile 2, information-sharing mode (line 4); true target acceleration (line 5); missile 1, purely delayed acceleration (line 6); and missile 2, purely delayed acceleration (line 7).

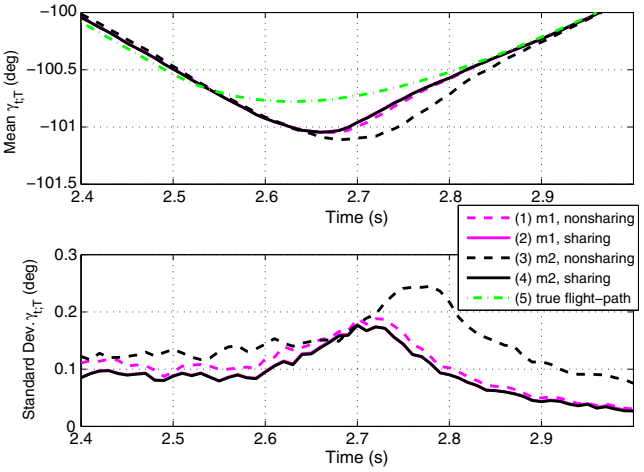

Fig. 10 Flight-path angle ($\gamma_{t;T}$) estimation at the switch ($t_{sw} = 2.5$ s), nonlinear MC simulation, both missiles, DGL1, and $\Delta X = 1500$ m: missile 1, information-nonsharing mode (line 1); missile 1, information-sharing mode (line 2); missile 2, information-nonsharing mode (line 3); missile 2, information-sharing mode (line 4); and true target flight-path angle (line 5).

acceleration, implemented in our deterministic model. It is evident that the acceleration delay of missile 2 improves in the sharing mode and almost does not change in missile 1, like our model predicts. We can also see that the improvement is similar to the improvement predicted by the deterministic model. Our deterministic model seems conservative relative to the mean target acceleration; however, taking into account the standard deviation and the fact that conservatism contributes to robustness, the pure delay model seems quite representative and useful for planning purposes.

Figure 10 compares the estimated target flight-path angle $\gamma_{t;T}$ of both missiles in the sharing and nonsharing modes. The figure also presents the true target flight-path angle. It is evident that the flight-path angle estimated by missile 2 improves in the sharing mode and almost does not change in missile 1. Note that this effect is not modeled in the deterministic model and its equivalent in the linear model is $\dot{\xi}_{t;i}$. The $\gamma_{t;T}$ error is a direct result of the $a_{t;T}$ delay because it is an integration of $a_{t;T}$ in the update stage of the filter [Eqs. (4)].

The guidance is governed by the ZEM. For the nonlinear DGL1, the ZEM is given by Eq. (51b) with $a^{n0}_{t;i}$ and $a^{n0}_{t;Ti}$ replaced by $a^{n}_{t;i}$ and $a^{n}_{t;Ti}$, respectively [Eq. (60)]. The Z_{PN} in Eq. (51b) is given by Eq. (57), yielding

$$Z_{DGL1} = Z_{PN} + Z_{ACC} \tag{64a}$$

$$Z_{PN} = -V_{\rho i} t^2_{go;i} \dot{\lambda}_{t;i} \tag{64b}$$

$$Z_{ACC} = a^n_{t;T} \tau^2_T \psi(\theta/\varepsilon) - a^n_{t;i} \tau^2_i \psi(\theta) \tag{64c}$$

In our head-on BMD scenario, $\cos(\delta_{t;Ti}) \approx 1$, $\cos(\delta_{t;i}) \approx 1$; thus, Eq. (60) leads to $a^n_{t;Ti} \approx a_{t;T}$, $a^n_{t;i} \approx a_{t;i}$. Therefore, the estimation error of Z_{ACC} is mainly a function of the target acceleration estimation error because we assume that the missile's own acceleration $a_{t;i}$ is known and the range ($\rho_{t;i}$) estimation error is relatively small at distances for which the target maneuver is effective. From Eq. (5) and $\cos(\delta_{t;Ti}) \approx 1$, $\cos(\delta_{t;i}) \approx 1$, we obtain $V_{\rho i} \approx -(V_{t;i} + V_T)$. Substituting this result and Eq. (58) into Eq. (64b) yields

$$Z_{PN} \approx \frac{\rho^2_{t;i}}{V_i + V_T} \dot{\lambda}_{t;i} \tag{65}$$

Because the range $\rho_{t;i}$ estimation error is relatively small at distances for which the target maneuver is effective, we can conclude that, at these distances, the estimation error in Z_{PN} is mainly a

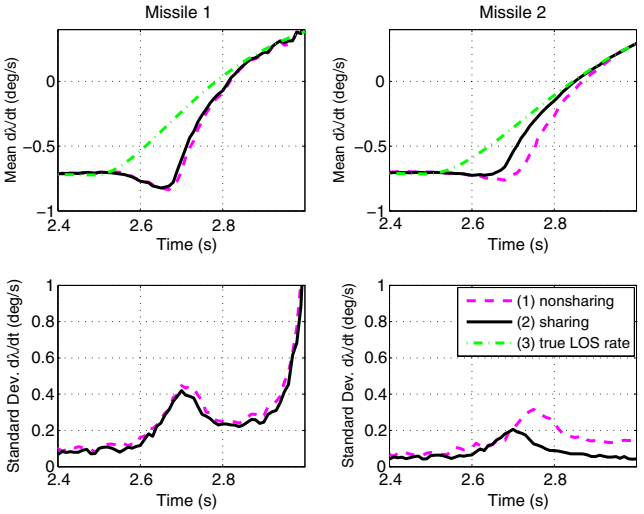

Fig. 11 LOS rate ($\dot{\lambda}_{t;i}$) estimation at the switch ($t_{sw} = 2.5$ s), nonlinear MC simulation, both missiles, DGL1, and $\Delta X = 1500$ m: information-nonsharing mode (line 1); information-sharing mode (line 2); and true LOS rate (line 3).

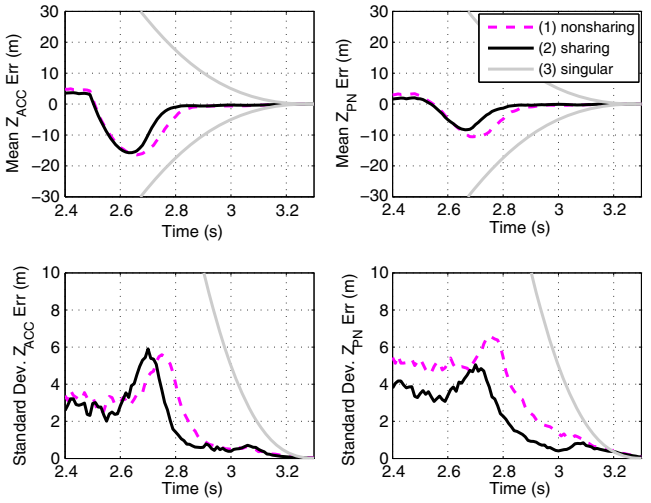

Fig. 13 ZEM estimation breakup (Z_{PN} and Z_{ACC}) at the switch ($t_{sw} = 2.5$ s), nonlinear MC simulation, missile 2, DGL1, and $\Delta X = 1500$ m: information-nonsharing mode (line 1); information-sharing mode (line 2); and singular region (line 3).

function of the estimation error in $\dot{\lambda}_{t;i}$ and the effect of the estimation error in $\gamma_{t;T}$ is reflected in $\dot{\lambda}_{t;i}$. Note that the estimation error in Z_{PN} is not reflected in the deterministic estimation model because only the estimated target acceleration time delay is considered by that model.

Figure 11 compares the estimated LOS rate $\dot{\lambda}_{t;i}$ of both missiles in the sharing and nonsharing modes. The figure also presents the true LOS rate. It is evident that the LOS rate estimated by missile 2 improves in the sharing mode and almost does not change in missile 1. Note the large error in the estimated $\dot{\lambda}_{t;i}$ at $t \approx 2.7$ s; this error is reflected in the Z_{PN} component of Z_{DGL1}.

Figure 12 compares the estimated ZEM (Z_{DGL1}) of missile 2 in the sharing and nonsharing modes. The figure also presents the true ZEM and the singular region for reference. It is evident that the target switch at $t_{sw} = 2.5$ s induces a very substantial error on the ZEM estimate. The ZEM estimate suffers a substantial delay, and its error is quite large compared to the size of the singular region. It is also apparent that the delay in the sharing mode is substantially lower than in the nonsharing mode. This difference constitutes the primary benefit of the cooperation and is the main reason for the improvement of the interception performance of missile 2, as will be demonstrated in Sec. VI.C.

Figure 13 presents the breakup of the ZEM estimation error of missile 2 into the proportional navigation (Z_{PN} Err.) and acceleration (Z_{ACC} Err.) components in the sharing and nonsharing modes. The figure also presents the size of the DGL1 singular region for reference. We present this figure to analyze the relative contribution of the components of the ZEM estimation error and to validate the assumption regarding the dominance of the acceleration component, used in the derivation of the deterministic estimation model. It is clear that both components of the ZEM have substantial errors. However, the acceleration component is the dominant one. Furthermore, because the target flight-path angle results from an integration of the target acceleration, and the flight-path angle estimation error is a dominant part of the estimation error of the proportional navigation component, the two estimated components of the ZEM have similar behaviors, which validates our estimation modeling approach. It is also apparent that the estimation errors of both components in the sharing mode are smaller, and they converge faster to zero than in the nonsharing mode.

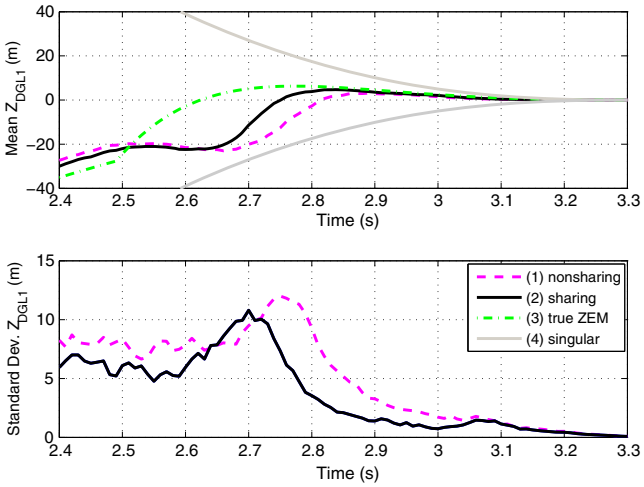

Fig. 12 ZEM (Z_{DGL1}) estimation at the switch ($t_{sw} = 2.5$ s), nonlinear MC simulation, missile 2, DGL1, and $\Delta X = 1500$ m: information-nonsharing mode (line 1); information-sharing mode (line 2); true ZEM (line 3); and singular region (line 4).

In terms of estimation performance enhancement, the main gain from information sharing is that of the trailing missile, as it benefits from the better information acquired by the leading missile. In particular, information sharing contributes mainly to lower the inherent time delay in estimating the target's acceleration and to decrease the estimation error of the target's flight-path angle, which is obtained from the (delayed) target acceleration estimate by integration. Predicted well by the deterministic model proposed in Sec. IV.B, the former has a major effect on decreasing the estimation error of the acceleration component of the ZEM, which is the ZEM's dominant error component. The latter contributes to lower the estimation error of the proportional navigation component of the ZEM.

C. Closed-Loop Guidance Performance

A Monte Carlo simulation study is used to compare the closed-loop interception performance of the missiles in the sharing and nonsharing modes. The target performs a bang–bang maneuver at its maximal acceleration of $a_T^{max} = 20$ g. The target starts at a maximal acceleration to one side, and it performs a maneuver switch at some point during the interception scenario. Two hundred Monte Carlo runs are performed at each switch time, and the switch times are performed at 0.05 s intervals from the launch time until the intercept time of the trailing missile (missile 2). A total of 13,600 runs are performed for each estimation mode.

Figure 14 presents the mean and the standard deviation of the miss distance of the leading missile (missile 1) in the sharing and nonsharing modes for a staggering of $\Delta X = 1500$ m. The predicted miss distance from the linear deterministic simulation is also presented for reference. In the deterministic estimation model, the estimation of the leading missile is not affected by the coopera-

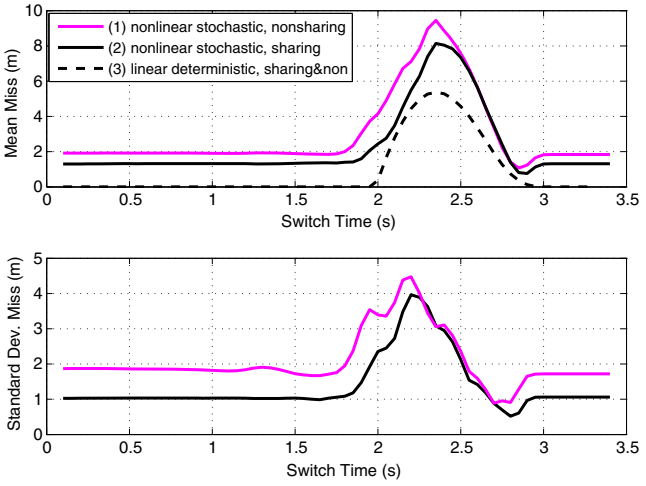

Fig. 14 Miss distance mean and standard deviation, linear deterministic and nonlinear MC simulation, missile 1, DGL1, and $\Delta X = 1500$ m: nonlinear stochastic simulation, information-nonsharing mode (line 1); nonlinear stochastic simulation, information-sharing mode (line 2); and linear deterministic simulation, information-sharing and nonsharing modes (line 3).

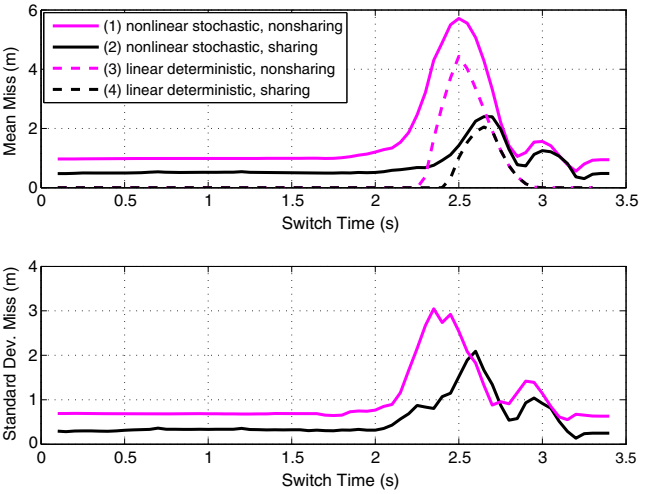

Fig. 16 Miss distance mean and standard deviation, linear deterministic and nonlinear MC simulation, team miss, DGL1, and $\Delta X = 1500$ m: nonlinear stochastic simulation, information-nonsharing mode (line 1); nonlinear stochastic simulation, information-sharing mode (line 2); linear deterministic simulation, information-nonsharing mode (line 3); and linear deterministic simulation, information-sharing mode (line 4).

tion; thus, only a single curve is presented for both modes. It is evident that the interception performance in the information-sharing mode is slightly better than in the nonsharing mode. This improvement can be attributed to the additional measurement from the trailing missile that, albeit of lower quality, still adds information. The deterministic model curve and the mean curve behave similarly; however, the deterministic model is more optimistic. This can be attributed to the partial estimation error modeling, which does not take into account the Z_{PN} estimation error. However, this similarity validates the linear deterministic model as a staggering planning tool. Note that the deterministic model predicts zero miss at early target maneuvers, which is not the case in the true stochastic setting. The miss in these early switches is small but, unlike the pure delay, which dies out and basically results in perfect information being passed to the guidance, in the stochastic setting, there are noises at each sample, which result in small miss distances due to state uncertainty.

Figure 15 presents the mean and the standard deviation of the miss distance of the trailing missile (missile 2) in the sharing and nonsharing modes for the same staggering. The predicted miss distance from the linear deterministic simulation is also presented for reference. It is apparent that the interception performance in the information-sharing mode is substantially better than in the nonsharing mode. This is the main benefit of the cooperation, as predicted and planned for. Like for missile 1, the deterministic model curves and the mean curves behave similarly and the deterministic model is optimistic. Note that, in the sharing mode, there is also a substantial improvement of the miss distances for early target switches. This improvement stems from the improved estimation of the ZEM just before intercept via the higher-quality measurements of missile 1.

Figure 16 presents the mean and the standard deviation of the team's miss distance in the sharing and nonsharing modes. It is obvious that the interception performance in the information-sharing mode is substantially better than in the nonsharing mode. Like in previous figures, the deterministic model curves and the mean curves

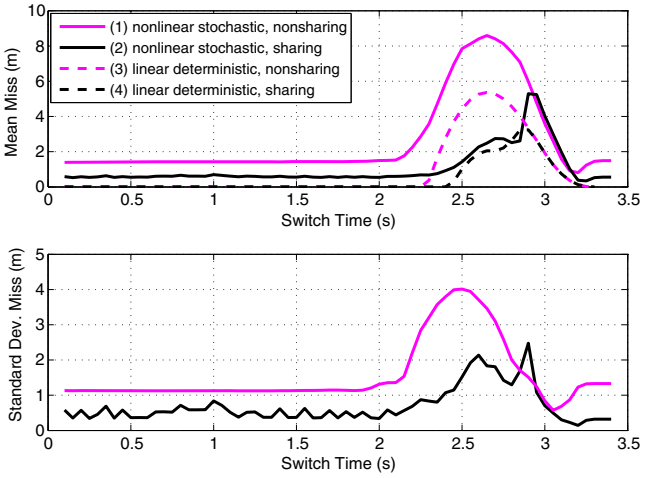

Fig. 15 Miss distance mean and standard deviation, linear deterministic and nonlinear MC simulation, missile 2, DGL1, and $\Delta X = 1500$ m: nonlinear stochastic simulation, information-nonsharing mode (line 1); nonlinear stochastic simulation, information-sharing mode (line 2); linear deterministic simulation, information-nonsharing mode (line 3); and linear deterministic simulation, information-sharing mode (line 4).

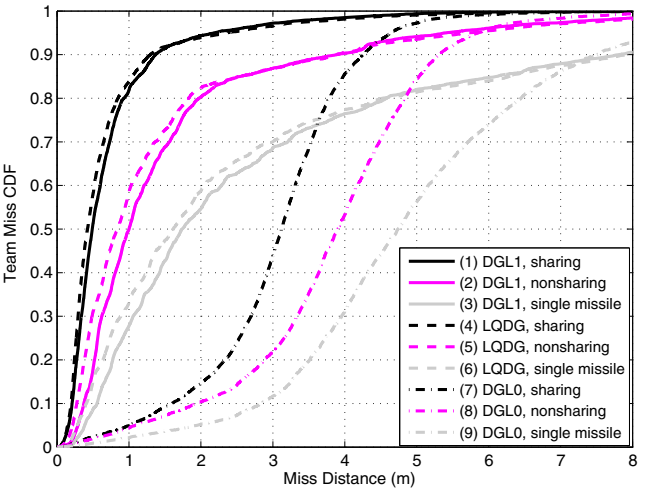

Fig. 17 Team miss distance CDF, nonlinear MC simulation, comparison of DGL1, LQDG, and DGL0; and $\Delta X = 1500$ m: DGL1, two missiles, information-sharing mode (line 1); DGL1, two missiles, information-nonsharing mode (line 2); DGL1, single missile (line 3); LQDG, two missiles, information-sharing mode (line 4); LQDG, two missiles, information-nonsharing mode (line 5); LQDG, single missile (line 6); DGL0, two missiles, information-sharing mode (line 7); DGL0, two missiles, information-nonsharing mode (line 8); and DGL0, single missile (line 9).

Table 1 Required warhead lethality ranges to ensure a 95% kill probability

Guidance law	Single missile, m	Two missiles nonsharing, m	Two missiles sharing, m
DGL1	10	5.4	2.2
LQDG	10.5	5.7	2.4
DGL0	9	5.8	4.7

are very similar and the deterministic model is optimistic. With this similarity, it is obvious that the deterministic model is a good tool for planning the staggering of the missiles. These results demonstrate a substantial reduction of the mean miss against an optimal single target switch from approximately 10 m (standard deviation ≈4.5 m) for a single missile shot (Fig. 14) to approximately 2.5 m (standard deviation ≈2 m) for a cooperative two-missile effort, which is a 75% reduction against an optimal target maneuver in a very difficult BMD scenario.

Figure 17 presents the team miss distance cumulative distribution function (CDF), which is defined on the minimum of the miss distances of both missiles for a uniformly distributed target switch time. The figure presents the performance in the sharing and nonsharing modes for three state-of-the-art guidance laws: DGL1, LQDG, and DGL0. The figure also presents the single missile CDF of the three guidance laws for reference. The required warhead lethality ranges to ensure a 95% kill probability are summarized in Table 1. Evidently, both the DGL1 and LQDG guidance laws perform very similarly, and both benefit significantly from information sharing. On the other hand, the DGL0 guidance law benefits relatively little from information sharing. This is because both DGL1 and LQDG use the estimates of the target acceleration, which substantially improves via staggering and information sharing. In fact, this state is the only one modeled in the deterministic model. On the other hand, DGL0 does not use the improved target acceleration estimate, and thus does not fully exploit the cooperation. The limited improvement in DGL0 stems from the improvement in the estimation of Z_{PN}, which is used by DGL0. It is also evident that a team of interceptors, in both cooperative and noncooperative modes, performs dramatically better than a single interceptor for all guidance laws.

As a direct result of its estimation performance improvement due to information sharing, the trailing missile also benefits the most in terms of interception performance. When the team uses guidance laws that use the target acceleration (e.g., DGL1 and LQDG), the trailing missile's performance dramatically improves as long as high-quality information from the leading missile is available (i.e., acceleration switch times before the leading missile passes the target), leading to a dramatic improvement in the team's interception performance: about 75% average miss distance reduction relative to a single interceptor pursuing an optimally evading target, or 50% reduction relative to a team that does not share information. Compared with the full nonlinear stochastic simulation, the linear deterministic model exhibits a similar qualitative behavior, thus corroborating its use as an engagement strategy planning tool.

VII. Conclusions

A novel cooperative tracking and interception strategy has been introduced that exploits information sharing and missile launch staggering. The key idea behind the approach is to exploit the superior information collected by the leading missile to improve the interception performance of the trailing missiles. To investigate and demonstrate the benefits of the new approach, an IMM estimator has been designed with two possible modes of operation: an information-sharing mode, in which each missile estimates the target states using its own and the other missiles' measurements; and an information nonsharing mode, in which each missile only uses its own measurements to estimate the target states. A linear deterministic model has been presented that closely approximates the full nonlinear stochastic model. The deterministic model is used as a tool to derive a staggering strategy for the interceptor team. The proposed estimation and staggering strategy has been extensively evaluated in Monte Carlo simulation, demonstrating significantly improved estimation performance and closed-loop interception performance in the information-sharing mode. It has been shown in simulation that the proposed approach dramatically improves the closed-loop interception performance when combined with guidance laws that use target acceleration.

References

[1] Zarchan, P., *Tactical and Strategic Missile Guidance*, 6th ed., Vol. 239, Progress in Astronautics and Aeronautics, AIAA, Reston, VA, 2012, pp. 13–34.

[2] Garber, V., "Optimum Intercept Laws for Accelerating Targets," *AIAA Journal*, Vol. 6, No. 11, 1968, pp. 2196–2198.

[3] Cottrell, G. R., "Optimal Intercept Guidance for Short-Range Tactical Missiles," *AIAA Journal*, Vol. 9, No. 7, 1971, pp. 1414–1415.

[4] Ben-Asher, J. Z., and Yaesh, I., *Advances in Missile Guidance Theory*, Vol. 180, Progress in Astronautics and Aeronautics, AIAA, Reston, VA, 1998, pp. 89–126.

[5] Gutman, S., "On Optimal Guidance for Homing Missiles," *Journal of Guidance and Control*, Vol. 3, No. 4, 1979, pp. 296–300.

[6] Shinar, J., *Solution Techniques for Realistic Pursuit-Evasion Games*, Academic Press, New York, 1981, pp. 63–124.

[7] Zarcham, P., "Representation of Realistic Evasive Maneuvers by Use of Shaping Filters," *Journal of Guidance and Control*, Vol. 2, No. 4, 1979, pp. 290–295.

[8] Magill, T. D., "Optimal Adaptive Estimation of Sampled Stochastic Processes," *IEEE Transactions on Automatic Control*, Vol. AC-10, No. 4, 1965, pp. 434–439.

[9] Sims, F. L., and Lainiotis, D. G., "Recursive Algorithm for the Calculation of the Adaptive Kalman Filter Weighting Coefficients," *IEEE Transactions on Automatic Control*, Vol. 14, No. 2, 1969, pp. 215–218.

[10] Oshman, Y., Shinar, J., and Avrash, W. S., "Using a Multiple Model Adaptive Estimator in Random Evasion Missile/Aircraft Encounter," *Journal of Guidance, Control, and Dynamics*, Vol. 24, No. 6, 2001, pp. 1176–1186.

[11] Shima, T., Oshman, Y., and Shinar, J., "Efficient Multiple Model Adaptive Estimation in Ballistic Missile Interception Scenarios," *Journal of Guidance, Control, and Dynamics*, Vol. 25, No. 4, 2002, pp. 667–675.

[12] Blom, H. A. P., "An Efficient Filter for Abruptly Changing Systems," *Proceedings of the 23rd Conference on Decision and Control*, IEEE, New York, 1984, pp. 656–658.

[13] Blom, H. A. P., and Bar-Shalom, Y., "The Interacting Multiple Model Algorithm for Systems with Markovian Switching Coefficients," *IEEE Transactions on Automatic Control*, Vol. 33, No. 8, 1988, pp. 780–783.

[14] Shinar, J., and Shima, T., "Nonorthodox Guidance Law Development Approach for Intercepting Maneuvering Targets," *Journal of Guidance, Control, and Dynamics*, Vol. 25, No. 4, 2002, pp. 658–666.

[15] Jeon, I. S., Lee, J. I., and Tahk, M. J., "Homing Guidance Law for Cooperative Attack of Multiple Missiles," *Journal of Guidance, Control, and Dynamics*, Vol. 33, No. 1, 2010, pp. 275–280. doi:10.2514/1.40136

[16] Ghosh, S., Ghose, D., and Raha, S., "Retro-PN Based Simultaneous Salvo Attack Against Higher Speed Nonmaneuvering Targets," *Advances in Control and Optimization of Dynamical Systems*, Vol. 3, No. 1, 2014, pp. 34–40.

[17] Meyer, I., Isaiah, P., and Shima, T., "On Dubins Paths to Intercept a Moving Target," *Automatica*, Vol. 53, March 2015, pp. 256–263. doi:10.1016/j.automatica.2014.12.039

[18] Shaferman, V., and Shima, T., "Cooperative Optimal Guidance Laws for Imposing a Relative Intercept Angle," *Journal of Guidance, Control, and Dynamics*, Vol. 38, No. 8, 2015, pp. 1395–1408.

[19] Shaferman, V., and Shima, T., "Cooperative Multiple-Model Adaptive Guidance for an Aircraft Defending Missile," *Journal of Guidance, Control, and Dynamics*, Vol. 33, No. 6, 2010, pp. 1801–1813. doi:10.2514/1.49515

[20] Shaferman, V., and Oshman, Y., "Cooperative Interception in a Multi-Missile Engagement," *AIAA Guidance, Navigation, and Control Conference*, AIAA Paper 2009-5783, 2009.

[21] Shima, T., "Optimal Cooperative Pursuit and Evasion Strategies Against a Homing Missile," *Journal of Guidance, Control, and Dynamics*,

Vol. 34, No. 2, 2011, pp. 414–425.
doi:10.2514/1.51765

[22] Mazor, E., Averbuch, A., Bar-Shalom, Y., and Dayan, J., "Interacting Multiple Model Methods in Target Tracking: A Survey," *IEEE Transactions on Aerospace and Electronic Systems*, Vol. 34, No. 1, 1998, pp. 103–123.

[23] Bar-Shalom, Y., Rong Li, X., and Kirubarajan, T., *Estimation with Applications to Tracking and Navigation*, Wiley, New York, 2001, pp. 453–460.

[24] Hexner, G., Weiss, H., and Dror, S., "Temporal Multiple Model Estimator for a Maneuvering Target," *AIAA Guidance, Navigation, and Control Conference*, AIAA Paper 2008-7456, 2008.